ORIGINAL RESEARCH

Validation of a surgical training model containing indocyanine green for near-infrared fluorescence imaging

Naoki Nishio MD, PhD[1] | **Sohei Mitani MD, PhD[2]** | **Kayo Sakamoto MD[2]** | **Gaku Morimoto MSC[3]** | **Sayaka Yokoi MD, PhD[1]** | **Mayu Shigeyama MD[1]** | **Akihisa Wada MD, PhD[1]** | **Nobuaki Mukoyama MD, PhD[1]** | **Eben L. Rosenthal MD[4]** | **Michihiko Sone MD, PhD[1]**

[1]Department of Otorhinolaryngology, Nagoya University Graduate School of Medicine, Nagoya, Aichi, Japan

[2]Department of Otolaryngology-Head and Neck Surgery, Ehime University Graduate School of Medicine, Toon, Ehime, Japan

[3]KOTOBUKI Medical Inc, Yashio, Saitama, Japan

[4]Department of Otolaryngology-Head and Neck Surgery, Vanderbilt University Medical Center, Nashville, Tennessee, USA

Correspondence
Naoki Nishio, Department of Otorhinolaryngology, Nagoya University Graduate School of Medicine, 65, Tsurumai-cho, Showa-ku, Nagoya, Aichi 466-8550, Japan.
Email: naokin@med.nagoya-u.ac.jp

Funding information
Hori Sciences Arts Foundation; Japan Society for the Promotion of Science, Grant/Award Number: JP22K09723

Abstract

Objective: To determine the efficacy of a surgical training model for fluorescence-guided cancer surgery and validate its utility to detect any residual tumors after tumor resection using electrocautery.

Methods: We developed surgical training models containing indocyanine green (ICG) for near-infrared (NIR) fluorescence imaging using a root vegetable organic material (konjac). After the fluorescence assessment for the models, the surgical simulation for fluorescence-guided cancer surgery using electrocautery was performed. ICG-containing tumors were divided into two surgical groups: "Enucleation" (removal of the entire visible tumor) and "Complete resection" (removal of the tumor with an appropriate 5-mm surgical margin).

Results: All 12 ICG-containing tumors were clearly visible from the normal view but not from the flipped view. The tumor resection time was significantly longer in the "Complete resection" group than in the "Enucleation" group ($p < .001$). The ICG-containing tumors showed a high tumor-to background ratio from the normal (average $= 45.8$) and flipped (average $= 19.2$) views, indicating that the models including ICG-containing tumors were useful for a surgical simulation in fluorescence-guided surgery. The average mean fluorescence intensity of the wound bed was significantly higher in the "Enucleation" group than in the "Complete resection" group ($p < .01$). No decrease in fluorescence signal was found in the wound bed even at 2 days postresection.

Conclusion: Our surgical training model containing a fluorescent agent is safe, inexpensive, not harmful for humans, and easy to dispose after use. Our model would be beneficial for surgeons to learn NIR fluorescence imaging and to accelerate fluorescence-guided cancer surgery into clinical application.

KEYWORDS
electrocautery, fluorescence-guided surgery, indocyanine green, near-infrared fluorescence imaging, surgical training

1 | INTRODUCTION

Fluorescence-guided surgery has emerged as a promising technique to overcome the limitations of human vision and to improve surgical precision during tumor resection. Recent clinical introduction and evaluation of fluorescently labeled imaging agents, such as the antiepidermal growth factor receptor (EGFR) antibodies or the antivascular endothelial growth factor antibody, have enabled us to differentiate the tumor regions from the surrounding normal tissues during surgery and demonstrated feasibility of obtaining a tumor-free margin resection in oncologic surgery.[1–5] In patients with head and neck squamous cell carcinomas (HNSCC), the EGFR is overexpressed in 90% of tumor tissue, making it an ideal candidate for targeting.[6] Our group has developed a surgical framework for margin assessment using near-infrared (NIR) fluorescence technique, in which ex vivo assessment of resected tumor specimens could visually point out where the closest margins are and allow surgeons to make a decision intraoperatively.[1,7,8] Moreover, other potential benefits of fluorescence-guided surgery have been reported, such as detection of secondary lesions, or residual disease in patients with HNSCC.[9]

To expand the clinical use of NIR fluorescence technique in the operating room, surgical training is essential to ensure the quality of surgery and critical for patients' safety. For complete tumor resection with a safe surgical margin, electrosurgery is a key surgical procedure in both open and minimally invasive surgeries. Tissue-like phantoms play a vital role in the development and validation for the fluorescence imaging technology. Phantoms are widely used for various purposes, such as initial tests of novel systems, routine quality control measurements, performance comparison of different systems, and signal-to-noise ratio optimization in existing systems.[10] Although several tissue-like phantoms for NIR fluorescence imaging were reported for the training of surgeons, the materials were composed of gelatin or agarose with hemoglobin,[11,12] resulting in lower usability and less stability of fluorescence signal for the surgical training. Importantly, the phantoms are clinically different from human tissues and not applicable for surgical training, especially using electrocautery. An appropriate surgical training model is required for NIR fluorescence imaging. Here, we have developed a surgical training model containing indocyanine green (ICG) for NIR fluorescence imaging using a root vegetable organic material (konjac), which is safe, inexpensive, and easy to transport. This study aimed to (1) determine the efficacy of a surgical training model for fluorescence-guided cancer surgery and (2) validate the utility of this model for detecting residual tumors after tumor resection using electrocautery.

2 | METHODS

2.1 | Materials

Flour and calcium hydroxide were obtained (Moteki Foods Engineering Co., Ltd., Gumma, Japan) and used as raw materials to make the surgical training models (Versatile Training Tissue (VTT), KOTOBUKI Medical Inc, Saitama, Japan), which are used for surgical simulation and training

and are made of edible ingredients. Color paint (Pentel Co., Ltd., Tokyo, Japan) was used to dye the models. Detailed methods for VTT models and its safety when using electrocautery in surgical simulation were previously described by us.[13] ICG (Diagnogreen®, Daiichi-Sankyo Pharma Co., Ltd, Tokyo, Japan) was obtained in this study and used as an ingredient for fluorescent imaging of VTT models.

2.2 | Preparation of VTT models with ICG-containing tumors

The experimental setup for VTT models with ICG-containing tumors as sketched in Figure 1. We referenced a process previously used to study image-guided drug delivery.[14] Konjac powder, salt, and color paint were dissolved in tap water, and calcium hydroxide was added to obtain the konjac paste (paste #1). Paste #2 was obtained by combining konjac powder, salt, and ICG in tap water with calcium hydroxide, resembling an ICG-containing tumor. Pastes #1 and #2 were placed in a rectangular mold and a dimpled mold, respectively, and these were then left to stand for at least 30 min to solidify. Paste #2 was formed into a hemisphere shape that could be removed from the dimpled mold so that it could be embedded in paste #1. The composed paste was kept in a low temperature environment ($-10°C$) for at least 30 min. Following this, the shaped model was dried to create a VTT model ($8 \times 5 \times 3$ cm^3, ~150 g). The final VTT model included two ICG-containing tumors, as shown in Figure 1.

2.3 | Surgical simulation for ICG-containing tumors using electrocautery

We performed the surgical simulation for fluorescence-guided cancer surgery using electrocautery (System 5000TM Electrosurgical Unit, Conmed, Inc., Largo, FL) in Nagoya University Medical xR Center. The workflow for the surgical procedures for the VTT models is illustrated in Figure 2. VTT models with ICG-containing tumors were placed on a metallic covered box and patient return electrodes were attached on the back to use electrocautery. ICG-containing tumors were divided into two surgical groups, which are as follows: "Enucleation" (removal of the entire visible tumor) and "Complete resection" (removal of the tumor with an appropriate 5-mm surgical margin). Surgical procedures were performed by a board-certified head and neck surgeon (N.N) in a similar way that is commonly performed for HNSCC in the operating room.

2.4 | Ex vivo assessment of NIR fluorescence imaging

Before tumor resection, the VTT models were imaged with the closed-field fluorescence imaging device (IVIS Lumina III, PerkinElmer, Inc, MA), which enables the measurement of the fluorescence intensity. After ICG-containing tumor resection, fluorescence intensity in the wound bed was measured from the normal and flipped views to assess

FIGURE 1 Schematic diagram of the procedure for preparing Pastes #1 and #2, the final paste, and a photograph of the prepared VTT model including ICG-containing tumors (scale bar: 5 cm). ICG, indocyanine green; VTT, versatile training tissue
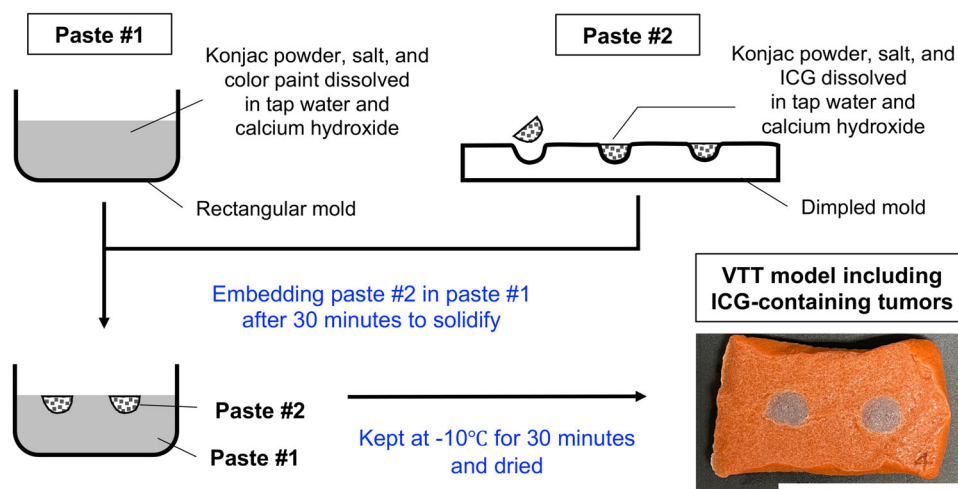

FIGURE 2 Surgical simulation of ICG-containing tumor using electrocautery. A board-certified head and neck surgeon performed two surgical procedures: "Enucleation" (removal of the entire tumor visibly) and "Complete resection" (removal of the tumor with an appropriately 5-mm surgical margin). After tumor resection, the tumor was cut into 5-mm slices to assess the peripheral and deep margins. ICG, indocyanine green
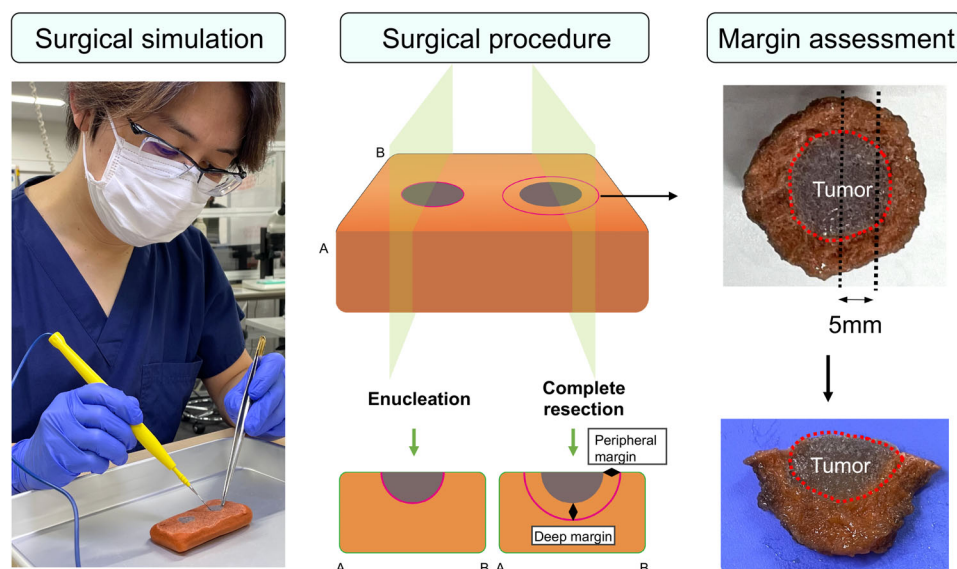
the residual fluorescence intensity of the VTT models. Thereafter, the resected ICG-containing tumors were cut into 5-mm thick slices as per the methods that we have previously described.[15] The fluorescence images of the wound bed and resected tumors were compared with images. Regions of interest (ROI) were drawn on the ICG-containing tumor, wound bed, and in the adjacent normal area using a fluorescence imaging device-integrated software (Living Image Software; PerkinElmer, Inc), and the mean fluorescence intensity (MFI) was defined. To exclude the effect of fluorescence signal in the analysis, the ROIs were set with a bright field image, in which the fluorescence signals were not displayed. Tumor-to-background ratio (TBR) was subsequently calculated by dividing target MFI by the adjacent normal MFI.[15]

2.5 | Statistical analyzes

During the surgical simulation, we measured the time for tumor resection, respective tumor diameters, volume, and surgical margins for the

"Enucleation" and "Complete resection" groups. Descriptive statistics were performed and figures were created using GraphPad Prism (version 6.0c, GraphPad Software, La Jolla, CA). A Mann–Whitney *U* test was used for comparison of the fluorescence intensity of the VTT models between the two groups. Statistical significance was set at a two-sided *p* value <.05.

3 | RESULTS

3.1 | Validation of the VTT model including ICG-containing tumors

Approximately 6 VTT models including 12 ICG-containing tumors were evaluated for surgical training. All 12 ICG-containing tumors were clearly visible from the normal view but not from the flipped view.

In the normal view, the average MFI for ICG-containing tumors was 17.3×10^8 a.u. (range $= 15.5 \times 10^8$–19.7×10^8 a.u.) and the

average MFI for background tissues was 0.4 $\times 10^8$ a.u. (range = 0.3×10^8–0.7×10^8 a.u.), as shown in Figure 3A. The ICG-containing tumors showed high TBR (average = 45.8, range = 32.1–62.3), indicating that the VTT models including ICG-containing tumors were available for a surgical simulation for FGS.

In the flipped view, the average MFI for ICG-containing tumors was 5.0×10^8 a.u. (range = 2.5×10^8–7.7×10^8 a.u.) and the average MFI for background tissues was 0.3×10^8 a.u. (range = 0.2×10^8–0.3×10^8 a.u.), as shown in Figure 3B. The ICG-containing tumors showed high TBR (average = 19.2; range = 10.4–33.7).
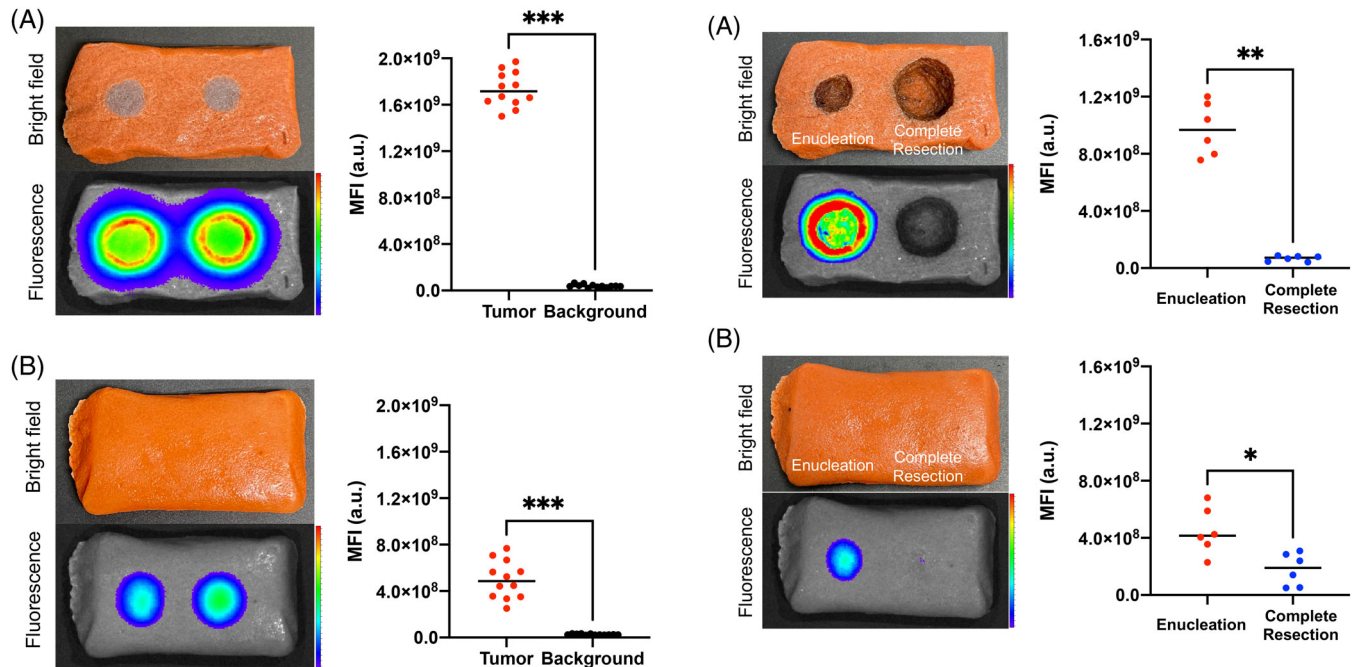

FIGURE 3 Validation for VTT models with ICG-containing tumors for NIR fluorescence imaging from the (A) normal and (B) flipped views. *p < .05, **p < .01, ***p < .001. ICG, indocyanine green; MFI, mean fluorescence intensity; VTT, versatile training tissue


FIGURE 4 Fluorescence signal for VTT models after resection of ICG-containing tumors from the (A) normal and (B) flipped views. *p < .05, **p < .01, ***p < .001. ICG, indocyanine green; MFI, mean fluorescence intensity; VTT, versatile training tissue

TABLE 1 Surgical simulation of ICG-containing tumors in the "Enucleation" and "Complete resection" groups

			Tumor				Margin	
Surgery	VTT	Time (seconds)	Major axis (mm)	Minor axis (mm)	Depth (mm)	Volume (mm³)	Peripheral (mm)	Deep (mm)
Enucleation	1	126	13	12	7	2286	N/A	N/A
	2	80	14	12	7	2462	N/A	N/A
	3	66	16	14	7	3282	N/A	N/A
	4	96	12	12	6	1809	N/A	N/A
	5	78	14	13	7	2667	N/A	N/A
	6	61	14	13	7	2667	N/A	N/A
Complete resection	1	284	22	23	14	14,829	5, 5	5
	2	200	22	18	12	9948	5, 5	6
	3	220	22	24	13	14,369	5, 5	5
	4	202	23	23	12	13,288	5, 5	7
	5	212	23	23	13	14,396	5, 5	7
	6	220	25	23	13	15,648	6, 6	7

Abbreviations: N/A, not applicable; VTT, versatile training tissue.

FIGURE 5 Changes in the fluorescence signal for the VTT models between Day 0 and Day 2 from the (A) normal and (B) flipped views. MFI, mean fluorescence intensity; NS, not significant; VTT, versatile training tissue
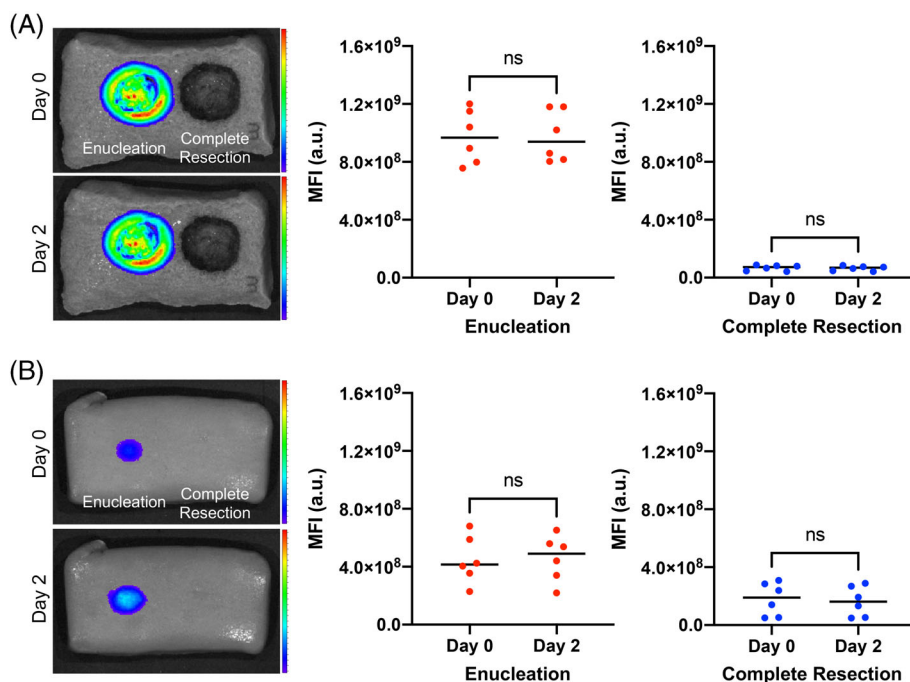
3.2 | Results of surgical simulation

Table 1 summarizes the results of the surgical simulation of 12 ICG-containing tumors from 6 VTT models in the "Enucleation" and "Complete resection" groups. The time for tumor resection of the "Complete resection" group was significantly longer than that of the "Enucleation" group (average = 84 s vs. 223 s; $p < .001$), because the ICG-containing tumors in the "Complete resection" group were resected from multiple views to obtain deep surgical margins. The peripheral and deep margins ranged from 5 to 7 mm in the "Complete resection" group, indicating a success of the complete tumor resection with a free margin using electrocautery.

3.3 | Detection of residual ICG-containing tumors in wound bed using NIR fluorescence imaging

After ICG-containing tumor resection, 6 VTT models were put in the closed field imaging device to evaluate the residual fluorescence intensity in the wound bed. In the normal view, the average MFI of the wound bed in the "Enucleation" group was significantly higher than that in the "Complete resection" group (average = 9.7×10^8 vs. 0.7×10^8 a.u.; $p < .01$), as shown in Figure 4A. The fluorescence intensity of the wound bed showed high TBR (average = 25.4; range = 20.9–37.9) in the "Enucleation" group and low TBR (average = 1.7; range = 0.8–2.5) in the "Complete resection" group. In the flipped view, the average MFI of the wound bed of the "Enucleation" group was significantly higher than that of the "Complete resection" group (average = 4.5×10^8 vs. 1.8×10^8 a.u.; $p < .05$), as shown in Figure 4B.

To evaluate the decrease of the fluorescence intensity in the wound bed, 6 VTT models were stored in the refrigerator in sealed, opaque plastic containers with limited light exposure for 2 days. Hereafter, the VTTs were re-imaged using the closed-field fluorescence imaging device from the normal and flipped views (Figure 5). In the normal view, the average MFI of the wound bed was not significantly different between at Day 0 and at Day 2 in the "Enucleation" (9.7×10^8 a.u. vs. 9.8×10^8, $p = .90$) and "Complete resection" (0.7×10^8 a.u. vs. 0.6×10^8, $p = .82$) groups. In the flipped view, similarly, the average MFI of the wound bed was not significantly different between at Day 0 and at Day 2 in the "Enucleation" (4.5×10^8 a.u. vs. 4.6×10^8, $p = .99$) and "Complete resection" group (1.8×10^8 a.u. vs. 1.6×10^8, $p = .69$) groups.

4 | DISCUSSION

As fluorescence-guided surgery expands broadly into the operating room,[16] surgical training models will be critical since fluorescence signal identified during real time is highly qualitative. In this study, we developed a surgical training model containing ICG, approved by the Food and Drug Administration for many biomedical applications, and first validated the efficacy of this model for FGS using electrocautery by qualitative measurement of fluorescence signal ex vivo. The ICG-containing tumors were visually removed in the "Enucleation" group, however, strong fluorescence signals remained in the wound bed. Ex vivo assessment of NIR fluorescence imaging revealed that a much higher TBR was obtained in the wound bed in the "Enucleation" group than that in the "Complete resection" group (average = 25.4 vs. 1.7). Moreover, the time for tumor resection of the "Complete resection" group was significantly longer than that of the "Enucleation" group.

To obtain safe surgical margins, the tumor should be resected from multiple views during the surgery, indicating that complete tumor resection strongly depends on the visual cues and experience in surgical techniques. Therefore, surgical training models containing ICG would be beneficial for teaching surgeons NIR fluorescence imaging and accelerating fluorescence-guided cancer surgery into clinical application. Recently, NIR fluorescence technology has emerged as a safe, feasible and useful tool that may facilitate more minimally invasive surgery, such as endoscopic and robotic surgeries. The evolution of robotics and surgical vision technology, such as anti-EGFR antibodies tagged with fluorescent dye and inherent autofluorescence, showed promise for improving positive surgical margin rates in head and neck surgery.[17] In our study, ex vivo assessment of whole tissue sample enabled us to detect the residual ICG-containing tumor in the wound bed after incomplete resection. For intraoperative decision making, a further study using ICG-containing tumor model is required both in ex vivo and in vivo settings. We believe that this pilot study would be a next step to the future precision surgery, such as endoscopic or robotic surgery, for decision making intraoperatively in HNSCC.

Expanded use of fluorescence-guided surgery with devices approved for human use with several fluorescence dyes, such as ICG, 5-aminolevulinic acid (5-ALA), fluorescein, IRDye800, has led to a range of commercial systems available.[18] ICG is by far the most widely used tissue perfusion agent within fluorescence-guided surgery due to its absorption and emission in the NIR range, low toxicity, and history of use within medicine for over half a century.[19] Currently, fluorescence-guided surgery with ICG is utilized in a broad range of clinical applications, such as assessment of blood perfusion or lymphatic drainage, and can contribute to the oncologic safety and reduction of complications.[20] 5-ALA is a nonfluorescent prodrug that leads to intracellular accumulation of fluorescent porphyrins and enables more complete resections of contrast-enhancing tumors in patients with malignant glioma.[21] Furthermore, in a recent study, 5-ALA has been used for transurethral tumor resection and cystoscopy in patients with bladder cancer.[22] NIR fluorescence imaging using tumor-targeted imaging agents has emerged as a promising and effective method of intraoperative cancer detection in many solid tumors.[23] In HNSCC, our group has developed a surgical framework for margin assessment using NIR fluorescence technique with an anti-EGFR antibody with IRDye800CW. Ex vivo assessment of resected tumor specimens could visually point out the closest margins and identify lymph nodes at risk of harboring metastatic disease.[1,2,7,8] Pafolacianine is also a fluorescent drug that targets folate receptors and has been recently approved for medical use in patients with ovarian cancer to help identify cancerous lesions during surgery. A recent randomized study in patients with ovarian cancer demonstrated the safety and effectiveness of pafolacianine for detecting the cancerous lesions that were not observed by standard visual or tactile inspection.[24] Among these fluorescent dyes commercially used in an operating room, we selected ICG and developed surgical models because of the low cost, wide usability, and safe properties. To standardize the NIR fluorescence technology for human use, a further study of training models containing different fluorescent agents is needed.

As the field of NIR fluorescence imaging expands, tissue-simulating phantoms with fluorescent dyes are essential and provide a major step toward standardizing performance characterization and cross-system comparisons for imaging devices.[25] Although several tissue-mimicking phantoms with ICG and IRDye800CW have been reported,[26,27] these phantoms are mainly used for standardization of the imaging device or fluorophore, but not for surgical training by surgeons. We focused on VTT models, which are made of konjac powder, salt, and calcium hydroxide and are used for surgical simulation.[13] Because VTT models use a root vegetable organic material (konjac), it is very easy to dispose after use. Moreover, we recently performed a surgical simulation for a variety of models (VTT, polyvinyl alcohol, porcine muscle, and liver) using electrocautery to identify chemical substances in smoke and demonstrated that surgical simulation with VTT models should be considered relatively safe.[13] In terms of fluorescence stability of VTT with ICG-containing tumors, no decrease of fluorescence was found in the wound bed even at 2 days after tumor resection. Therefore, the VTT model with ICG-containing tumors has strong advantages for use during surgical training in fluorescence-guided surgery, including its safety, low cost, easy transportation, and fluorescence stability. Moreover, HNSCC is often irregular or asymmetrical in shape with notched borders. Thus, advanced tumor models with one or two spikes projecting deeply into the mold would be more beneficial for advanced residents or fellows. Despite the fact that "on-the-job" training (coincidental experience) is the basis of acquiring surgical skills for young surgeons, "off-the-job" training (planned experience) is essential to acquire advanced surgical skills and to motivate them to learn surgical techniques.[28] VTT models with ICG-containing tumors could be a very useful tool for teaching surgeons how to remove the tumor by using electrocautery as "off-the-job" training.

This study has a few limitations. In general, tumor resection is considered adequate when the surgical margins are >5 mm on final histology in HNSCC and complete tumor resection is not easy for young surgeons. Especially in tumors in the deep regions. Due to a proof-of-concept study, only a board-certified head and neck surgeon performed the surgical resection for the VTT model, resulting in reliable surgical margins (5–7 mm) both in the peripheral and deep regions. The surgical training using VTT model should be done by both experts and young surgeons and the comparison of surgical margins would be useful to determine the efficacy of this training. To develop the surgical training curriculum for young surgeons, the fundamental skills should be verbalized, categorized, and evaluated via expert consensus.[28,29] To standardize the quality of fluorescence-guided surgery and improve patient outcomes, further studies by experts, residents, and medical students from multiple institutions should be performed and the VTT model needs repetition of implementation and evaluation.

5 | CONCLUSION

Our surgical training model containing a fluorescent agent is safe, inexpensive, not harmful for humans, and easy to dispose after use. We first validated the efficacy of this model for FGS using

electrocautery. Fluorescence-based surgical training would be beneficial for surgeons to accelerate fluorescence-guided cancer surgery into clinical application.

AUTHOR CONTRIBUTIONS

Naoki Nishio and Sohei Mitani designed the study, analyzed the results, and drafted the manuscript. All authors contributed to the conception and design of the study. Eben L. Rosenthal and Michihiko Sone supervised the study and assisted in the preparation of the manuscript. All authors reviewed and approved the final version of the manuscript.

CONFLICT OF INTEREST

Eben L. Rosenthal has institutional equipment loans from LICOR Biosciences and Stryker. All other authors declare no conflict of interest.

ORCID

Naoki Nishio https://orcid.org/0000-0003-1495-0376
Michihiko Sone https://orcid.org/0000-0001-7380-610X

REFERENCES

1. van Keulen S, Nishio N, Birkeland A, et al. The sentinel margin: intraoperative ex vivo specimen mapping using relative fluorescence intensity. *Clin Cancer Res*. 2019;25(15):4656-4662.
2. Nishio N, van den Berg NS, van Keulen S, et al. Optical molecular imaging can differentiate metastatic from benign lymph nodes in head and neck cancer. *Nat Commun*. 2019;10(1):5044.
3. Lu G, van den Berg NS, Martin BA, et al. Tumour-specific fluorescence-guided surgery for pancreatic cancer using panitumumab-IRDye800CW: a phase 1 single-Centre, open-label, single-arm, dose-escalation study. *Lancet Gastroenterol Hepatol*. 2020;5(8):753-764.
4. Koller M, Qiu SQ, Linssen MD, et al. Implementation and benchmarking of a novel analytical framework to clinically evaluate tumor-specific fluorescent tracers. *Nat Commun*. 2018;9(1):3739.
5. de Jongh SJ, Tjalma JJJ, Koller M, et al. Back-table fluorescence-guided imaging for circumferential resection margin evaluation using bevacizumab-800CW in patients with locally advanced rectal cancer. *J Nucl Med*. 2020;61(5):655-661.
6. Grandis JR, Tweardy DJ. Elevated levels of transforming growth factor alpha and epidermal growth factor receptor messenger RNA are early markers of carcinogenesis in head and neck cancer. *Cancer Res*. 1993;53(15):3579-3584.
7. Krishnan G, van den Berg NS, Nishio N, et al. Fluorescent molecular imaging can improve intraoperative sentinel margin detection in oral squamous cell carcinoma. *J Nucl Med*. 2022;63(7):262235. doi:10.2967/jnumed.121.262235
8. Fakurnejad S, Krishnan G, van Keulen S, et al. Intraoperative molecular imaging for ex vivo assessment of peripheral margins in oral squamous cell carcinoma. *Front Oncol*. 2019;9:1476.
9. van Keulen S, Nishio N, Fakurnejad S, et al. The clinical application of fluorescence-guided surgery in head and neck cancer. *J Nucl Med*. 2019;60(6):758-763.
10. Pogue BW, Patterson MS. Review of tissue simulating phantoms for optical spectroscopy, imaging and dosimetry. *J Biomed Opt*. 2006;11(4):041102.
11. De Grand AM, Lomnes SJ, Lee DS, et al. Tissue-like phantoms for near-infrared fluorescence imaging system assessment and the training of surgeons. *J Biomed Opt*. 2006;11(1):014007.
12. Pleijhuis RG, Langhout GC, Helfrich W, et al. Near-infrared fluorescence (NIRF) imaging in breast-conserving surgery: assessing intraoperative techniques in tissue-simulating breast phantoms. *Eur J Surg Oncol*. 2011;37(1):32-39.
13. Morimoto G, Kawahira H, Takayama S, Lefor AK. Chemical components of smoke produced from versatile training tissue models using electrocautery. *Simul Healthc*. 2022;17(1):29-34.
14. Zhu Z, Si T, Xu RX. Microencapsulation of indocyanine green for potential applications in image-guided drug delivery. *Lab Chip*. 2015;15(3):646-649.
15. Nishio N, van den Berg NS, van Keulen S, et al. Optimal dosing strategy for fluorescence-guided surgery with panitumumab-IRDye800CW in head and neck cancer. *Mol Imaging Biol*. 2020;22(1):156-164.
16. Zhang RR, Schroeder AB, Grudzinski JJ, et al. Beyond the margins: real-time detection of cancer using targeted fluorophores. *Nat Rev Clin Oncol*. 2017;14(6):347-364.
17. Holsinger FC, Birkeland AC, Topf MC. Precision head and neck surgery: robotics and surgical vision technology. *Curr Opin Otolaryngol Head Neck Surg*. 2021;29(2):161-167.
18. Koch M, Ntziachristos V. Advancing surgical vision with fluorescence imaging. *Annu Rev Med*. 2016;67:153-164.
19. Zelken JA, Tufaro AP. Current trends and emerging future of indocyanine green usage in surgery and oncology: an update. *Ann Surg Oncol*. 2015;22(Suppl 3):S1271-S1283.
20. Knospe L, Gockel I, Jansen-Winkeln B, et al. New intraoperative imaging tools and image-guided surgery in gastric cancer surgery. *Diagnostics (Basel)*. 2022;12(2):507.
21. Stummer W, Pichlmeier U, Meinel T, et al. Fluorescence-guided surgery with 5-aminolevulinic acid for resection of malignant glioma: a randomised controlled multicentre phase III trial. *Lancet Oncol*. 2006;7(5):392-401.
22. Kelloniemi E, Jarvinen R, Hellstrom P, et al. Repeated 5-aminolevulinic acid instillations during follow-up in non-muscle-invasive bladder cancer: a randomized study. *In Vivo*. 2021;35(3):1561-1568.
23. Mieog JSD, Achterberg FB, Zlitni A, et al. Fundamentals and developments in fluorescence-guided cancer surgery. *Nat Rev Clin Oncol*. 2022;19(1):9-22.
24. Voelker R. Lighting the way for improved detection of ovarian cancer. *JAMA*. 2022;327(1):27.
25. Ruiz AJ, Wu M, LaRochelle EPM, et al. Indocyanine green matching phantom for fluorescence-guided surgery imaging system characterization and performance assessment. *J Biomed Opt*. 2020;25(5):1-15.
26. Liu Y, Ghassemi P, Depkon A, et al. Biomimetic 3D-printed neurovascular phantoms for near-infrared fluorescence imaging. *Biomed Opt Express*. 2018;9(6):2810-2824.
27. Samkoe KS, Bates BD, Tselepidakis NN, et al. Development and evaluation of a connective tissue phantom model for subsurface visualization of cancers requiring wide local excision. *J Biomed Opt*. 2017;22(12):1-12.
28. Sato E, Mitani S, Nishio N, et al. Development of proficiency-based knot-tying and suturing curriculum for otolaryngology residents: a pilot study. *Auris Nasus Larynx*. 2020;47(2):291-298.
29. Mitani S, Nishio N, Kitani T, et al. Verbalization, categorization, and evaluation of fundamental surgical skills: an expert consensus in open head and neck surgery. *Ann Surg Open*. 2021;2(2):e059.